ACS OMEGA

http://pubs.acs.org/journal/acsodf

Article

Quantum Chemical Study on Mefenamic Acid Polymorphic Forms

Svitlana V. Shishkina,* Yevhenii A. Vaksler, Irina S. Konovalova, Victoriya V. Dyakonenko, and Victoriya V. Varchenko

Cite This: *ACS Omega* 2022, 7, 17544−17554

Read Online

ACCESS | Metrics & More | Article Recommendations | Supporting Information

ABSTRACT: Three polymorphic structures of mefenamic acid, which is a very popular drug, have been studied using quantum chemical methods. It has been shown that the centrosymmetric dimer formed due to two O−H···O hydrogen bonds is a complex building unit in all of the polymorphic structures under study. On the basis of an analysis of the pairwise interaction energies between molecules, the polymorphic forms **I** and **II** are classified as columnar-layered while the polymorphic form **III** has a columnar structure. The stabilities of the three polymorphic forms of mefenamic acid under ambient conditions (**I** > **II** > **III**) correlate with the degree of anisotropy of the interaction energies between columns (primary basic structural motifs) formed due to stacking interactions. The shear deformation modeling of strongly bound layers in all of the polymorphic structures has not revealed any possibility for deformation of the crystal structure. The construction of the shift energy profiles and calculation of the energy barriers for the displacement along the (100) crystallographic plane in the [100], [010], and [011] crystallographic directions make it possible to explain the experimental data obtained for commercially available polymorphic structure **I** in a diamond anvil cell. The absence of any local minimum near the starting point on the shift energy profile and the extremely high energy barrier can be considered as criteria for the impossibility of a crystal structure deformation under pressure.

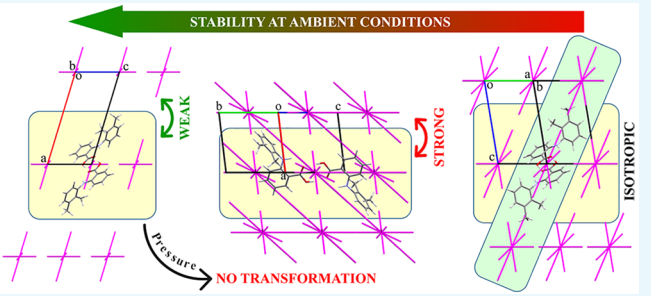

INTRODUCTION

Mefenamic acid (MA, 2-[(2,3-dimethylphenyl)amino]benzoic acid) is a fenamate derivative used as a nonsteroidal anti-inflammatory drug.[1] The mefenamic acid molecule is conformationally flexible and has been studied theoretically by both molecular mechanics and semiempirical methods[2,3] as well as *ab initio* calculations.[4] The ability to change its conformation is caused by the rotation of a dimethylphenyl group around the C_{ar}−N bond. It was shown that the relaxed conformational scan for this process depends crucially on the calculation method used.[4] Mefenamic acid as a drug is manufactured in a solid state. It possesses low solubility in water, which restricts its utility in clinical practice. Consequently, this problem needs to be tackled to improve the bioavailability of mefenamic acid.

For a long time, only two polymorphic forms of MA were known.[5−7] These polymorphs can be obtained from different solvents,[8,9] and their solubility and dissolution rate were studied thoroughly.[10−12] Both polymorphic structures were characterized by different physicochemical methods,[13−17] and the thermal conversion of mefenamic acid from its polymorphic form **I** to polymorphic form **II** was revealed and studied by IR spectroscopy.[18] However, the polymorphic form **I** of mefenamic acid proved to be more stable than form **II** under ambient conditions, which causes a slow transformation of polymorph **II** to polymorph **I**.[19,20] The mechanism of this thermally dependent reversible polymorphic transition remains unclear due to the fact that the mefenamic acid molecule is disordered in the polymorphic form **II**. The intricate disorder of mefenamic acid was solved in a more correct way later.[21] The polymorphic form **I** is known to be commercially available; thus, its behavior under pressure influence was studied.[22] The new polymorphic form **III** of mefenamic acid was reported recently, and a comprehensive study of the molecular and crystal structures of the three polymorphic forms has been performed.[23] In addition, the thermal phase transitions of three polymorphic forms as well as their relative stabilities at different temperatures were reported.[24] However, a geometrical characteristic analysis of intermolecular interactions is insufficient in many cases and cannot explain the properties of a solid form that correlate with the anisotropy of a crystal structure.

An analysis of the pairwise interaction energies between molecules turned out to be more efficient. This approach makes it possible to take into account not only strong

Received: December 9, 2021
Accepted: April 28, 2022
Published: May 16, 2022

intermolecular interactions, such as hydrogen bonds, but also weak interactions, such as X−H···Lp, X−H···π, and halogen bonds, as well as nonspecific interactions.[25,26] The study of an "energetic" structure of molecular crystals also allows discussing various properties of a crystal form, including the relative stabilities of polymorphic structures. Moreover, the results of such a study can be used for the further modeling of a crystal structure deformation under the influence of pressure.[27,28]

In the present study, we analyze three polymorphic modifications of mefenamic acid from an energetic viewpoint to explain their capability to be deformed.

RESULTS AND DISCUSSION

Conformational Analysis. It is well-known that mefenamic acid is a conformationally flexible molecule. Theoretically, its flexibility can be caused by the rotation around three single bonds, C6−C7, C1−N1, and N1−C8 (Figure 1).[23]

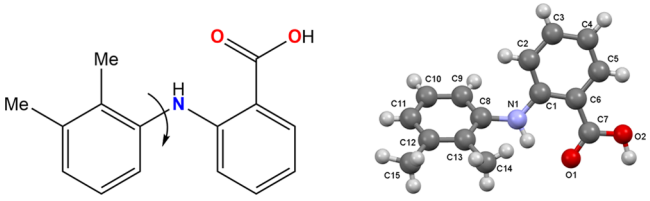

Figure 1. (left) Scheme of the mefenamic acid structure. (right) Molecular structure of mefenamic acid according to X-ray diffraction data with the numbering scheme.

However, the rotation about the C6−C7 and C1−N1 bonds is hindered due to the formation of a N1−H···O1 intramolecular hydrogen bond. The only way to change the conformation of mefenamic acid is rotation around the N1−C8 bond.

Previously, relaxed conformational scanning around the N1−C8 bond was performed and it was shown that the energy profile depends on the level of computation.[4] The sole 0−150° diapason of the C_{ar}−N−C_{ar}−C_{ar} torsion angle change was discussed in previous works;[4,29] thus, we revisited the energy profile for full rotation (360°) around the N1−C8 bond to study all possible conformations of mefenamic acid. As can be seen from Figure 2, two pairs of symmetrical conformations with C1−N1−C8−C13 torsion angle values of about ±60 and ±140° correspond to the minima on this energy profile. The energy barriers for the rotation about the N1−C8 bond were estimated to be 4.9 and 8.5 kcal/mol, respectively.

The energy profile for full rotation around the N1−C8 bond proved to be slightly unexpected. Depending on the direction of the C_{ar}−N−C_{ar}−C_{ar} torsion angle change (with a step size of +10 or −10°), an abrupt change in energy was found between −210 and −220° or between +210 and +220° (Figure 2). Since the transition state have to be about 180° in the relaxed scan, such a peak appears as an artifact of the scanning procedure. However, a detailed study of the molecular geometry in the diapason of the C_{ar}−N−C_{ar}−C_{ar} torsion angle changes from ±150 up to ±230° showed an extremely strong steric repulsion within the molecule (Table S1). This repulsion increases with the change of the torsion angle up to ±210° and decreases sharply in the area between ±210 and ±220°. It should also be noted that the decrease in short noncovalent distances is monotonic in the area with a C_{ar}−N−C_{ar}−C_{ar} torsion angle value from ±150 up to ±180°. The

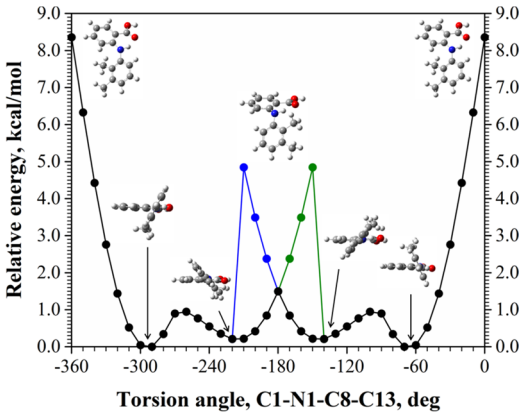

Figure 2. Energy profiles of the rotation around the N1−C8 bond in two opposite directions in mefenamic acid according to quantum chemical calculations by the m06-2x/cc-pVTZ method. The conformations of the mefenamic acid molecule in equilibrium and transition states are presented.

change in the torsion angle from ±180 up to ±230° is accompanied by an increase of one part of the short distances and a decrease of another part and *vice versa* (Table S1). Such an unusual nonmonotonic change of short noncovalent distances leads to an increase in molecular energy and indicates attempts of a molecule to compensate for the strong steric repulsion, which acts like a switch in the conformational transition. In addition, these results explane the small diapason of the C_{ar}−N−C_{ar}−C_{ar} torsion angle change studied earlier.[4,29]

An analysis of the mefenamic acid molecular structure in the three polymorphic forms showed that this molecule is found in a nonequilibrium conformation in the crystal phase (Table 1).

Table 1. Selected Geometrical Parameters for the Molecular Structures of Mefenamic Acid According to Experimental X-ray Data

		N1−H···O1 intramolecular hydrogen bond	
polymorphic form	C1−N1−C8−C13 torsion angle, deg	H···A, Å	D−H···A, deg
I[5]	−119.99	1.89	137.3
II, conformer **A**[21]	−107.69	1.97	135.5
II, conformer **B**[21]	87.08	2.01	133.9
III[23]	−80.82	2.01	133.6

This can be due to the influence of intermolecular interactions and packing effects on the molecule. Moreover, the molecule of mefenamic acid is disordered due to the rotation of a dimethylphenyl fragment around the N1−C8 bond in the polymorphic structure **II**.[21] This means that two conformers (**A** and **B**) of mefenamic acid are present in the crystal phase.

Crystal Structure Analysis of Mefenamic Acid Polymorphic Structures. Mefenamic acid contains a carboxylic group that can provide the formation of supramolecular synthons of two types: i.e., a centrosymmetric synthon bound by two O−H···O hydrogen bonds or a linear synthon bound by one O−H···O hydrogen bond.[30,31] The centrosymmetric dimer, in which molecules are bound by two O−H···O′ intermolecular hydrogen bonds, is found in all three polymorphic structures of mefenamic acid (Figure 3 and Table 2). The stacking interaction between benzoic acid fragments of

https://doi.org/10.1021/acsomega.1c06967
ACS Omega 2022, 7, 17544−17554

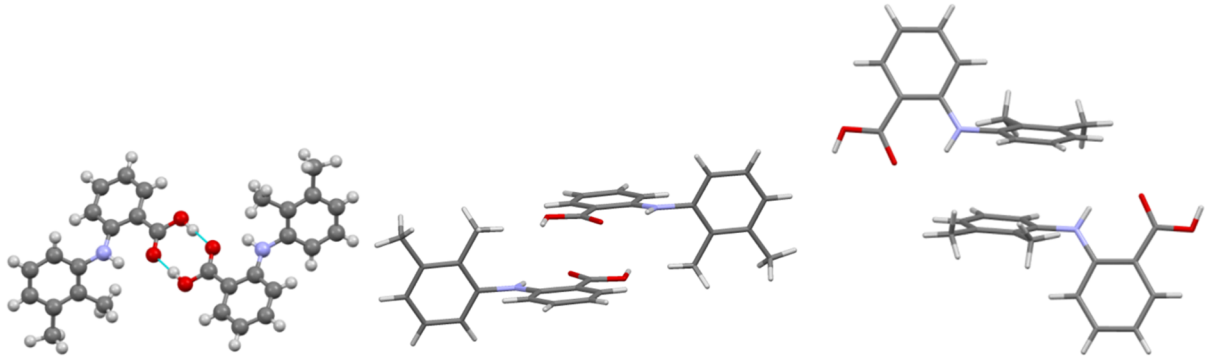

Figure 3. (left) Centrosymmetric dimer and (middle) stacked dimer (in the middle) for all three polymorphic structures as well as (right) another stacked dimer found in the polymorphic form **II**.

Table 2. Intermolecular Interactions and Their Geometric Characteristics in Mefenamic Acid Polymorphic Crystals of I–III

		geometrical characteristics	
interaction	symmetry operation	H···A, Å	D–H···A, deg
	Polymorph **I**		
O1–H···O2′	$-x, 1-y, -z$	1.69	174
stacking between benzoic acid groups	$-x, -y, -z$	distance between mean planes 3.42 Å, plane to plane shift 1.478 Å	
	Polymorph **II**, Conformer **A**		
O1–H···O2′	$-x, 2-y, 1-z$	1.73	168
C3–H···C12′ (π)	$-x, 1-y, 2-z$	2.78	149
C14–H···C3′ (π)	$1+x, y, z$	2.89	133
	Polymorph **II**, Conformer **B**		
O1–H···O2′	$-x, 2-y, 1-z$	1.97	171
C3–H···C12′ (π)	$-x, 1-y, 2-z$	2.88	134
C14–H···O1′ (π)	$-x, 2-y, 2-z$	2.65	125
C10–H···C9′ (π)	$1+x, y, z$	2.82	158
C10–H···C10 (π)	$1+x, y, z$	2.85	158
stacking between benzoic acid groups	$-x, 1-y, 1-z$	distance between mean planes 3.44 Å, plane to plane shift 1.732 Å	
stacking between dimethylphenyl groups	$1-x, 2-y, 2-z$	distance between mean planes 3.48 Å, plane to plane shift 1.309 Å	
	Polymorph **III**		
O1–H···O2′	$1-x, 1-y, -z$	1.69	172
stacking between benzoic acid groups	$-x, 2-y, -z$	distance between mean planes 3.48 Å, plane to plane shift 0.545 Å	

neighboring molecules is also present in the polymorphic structures under study. In contrast to polymorphs **I** and **III**, a large number of C–H···π′ hydrogen bonds as well as stacking interactions between dimethylphenyl fragments were revealed in the polymorphic structure **II** (Figure 3 and Table 2).

It should be noted that an analysis of intermolecular interactions in a traditional way did not make it possible to discuss the crystal packing anisotropy in the polymorphic structures under study. Therefore, we applied an approach to the crystal structure analysis based on the study of the pairwise interaction energies between molecules proposed previously.[32−34] When the presence of two conformers in the polymorphic form **II** was taken into account, the packing of each conformer (**A** and **B**) was studied separately and compared to check the applicability of the aforementioned method to the disordered structures.

At the first stage of the present study a molecule was used as a basic building unit (MBU_0) for an analysis of pairwise interaction energies. The first coordination sphere of the basic MBU_0 contains 14 neighboring molecules in structures **I** and **III**, while the numbers of neighboring molecules are different for conformers **A** (13) and **B** (16) in the structure **II**. The total interaction energies of the basic MBU_0 with its first coordination sphere is −76.8 kcal/mol in structure **I**, −72.5 kcal/mol for conformer **A** and −72.9 kcal/mol for conformer **B** in structure **II**, and −73.1 kcal/mol in the structure **III**. The basic molecule forms the strongest interaction with only one neighboring molecule in all of the structures under study (Table 3). Hence, this centrosymmetric dimer should be considered as a complex dimeric building unit (DBU).

All the procedures carried out for a molecule as a simple building unit were repeated for a centrosymmetric dimer as a complex building unit. The first coordination sphere of the DBU_0 contains 16 neighboring DBU_is in structures **I** and **III** and proved to be different for conformers **A** and **B** in structure **II** (14 and 18 neighbors for conformers **A** and **B**, respectively). The total interaction energies of the DBU_0s with their first coordination sphere are −118.5 kcal/mol in structure **I**, −113.0 kcal/mol for conformer **A** and −115.6 kcal/mol for conformer **B** in structure **II**, and −116.2 kcal/mol in structure **III**.

The basic DBU_0 forms two strongest interactions in opposite directions in structure **I** (Table 4). Dimers are bound by stacking interactions between benzoic acid fragments in these directions. As a result, a column (Figure 4) should be recognized as a primary basic structural motif (BSM_1) in the polymorphic form **I**. The interaction energy of the DBU_0 with its neighbors within such a column is −36.5 kcal/mol.

The interaction energies between neighboring columns are not equal. The DBUs belonging to the basic column interact more strongly with two neighboring columns lying within the (100) crystallographic plane (Figure 4). The interaction energy of the DBU_0 within this layer is −89.8 kcal/mol, while the interaction energy between adjacent layers is −28.7 kcal/mol. Consequently, a layer should be considered as a secondary basic structural motif (BSM_2) of structure **I**. Thus, the results of pairwise interaction energy calculations showed that the polymorphic structure **I** of mefenamic acid can be classified as columnar-layered.

https://doi.org/10.1021/acsomega.1c06967
ACS Omega 2022, 7, 17544−17554

Table 3. Symmetry Codes, Bonding Types, Interaction Energies of the Basic Molecular BU_0s with Neighboring Ones (E_{int}, kcal/mol) with the Highest Values (More Than 10% of the Total Interaction Energy) and the Contributions of These Energies to the Total Interaction Energy (%) in the Polymorphic Structures I–III

dimer	symmetry operation	E_{int}, kcal/mol	contribution to the total interaction energy, %	interaction type
		Polymorph **I**		
I_d1	$-x, 1-y, -z$	−17.4	22.7	O–H···O
I_d2	$1-x, -y, -z$	−9.6	12.6	nonspecific
I_d3	$-x, -y, -z$	−8.2	10.7	stacking between benzoic acid groups
		Polymorph **II**, Conformer **A**		
IIA_d1	$-x, 2-y, 1-z$	−17.1	23.6	O–H···O
IIA_d2	$1-x, 2-y, 2-z$	−12.6	17.4	stacking between dimethylphenyl groups
IIA_d3	$-x, 1-y, 2-z$	−8.6	11.9	C–H
IIA_d4	$-x, 1-y, 1-z$	−8.4	11.6	stacking between benzoic acid groups
		Polymorph **II**, Conformer **B**		
IIB_d1	$-x, 2-y, 1-z$	−16.0	21.9	O–H···π···O
IIB_d2	$1-x, 2-y, 2-z$	−12.3	16.9	stacking between dimethylphenyl groups
IIB_d3	$-x, 1-y, 1-z$	−8.7	11.9	stacking between benzoic acid groups
		Polymorph **III**		
III_d1	$1-x, 1-y, -z$	−17.7	24.3	O–H···O
III_d2	$-x, 2-y, -z$	−9.4	12.9	stacking between benzoic acid groups
III_d3	$-1-x, 2-y, 1-z$	−8.5	11.6	nonspecific
III_d4	$-x, 1-y, 1-z$	−7.6	10.4	nonspecific

Table 4. Symmetry Codes, Bonding Types, Interaction Energies of the Basic Dimeric BU_0s with Neighboring Ones (E_{int}, kcal/mol) with the Highest Values (More Than 5% of the Total Interaction Energy) and the Contributions of These Energies to the Total Interaction Energy (%) in the Polymorphic Structure I

dimer	symmetry operation	E_{int}, kcal/mol	contribution to the total interaction energy, %	interaction type
I_dd1	$x, 1+y, z$	−18.3	15.4	stacking between benzoic acid groups
I_dd2	$x, -1+y, z$	−18.3	15.4	
I_dd3	$x, y, 1+z$	−13.4	11.3	nonspecific
I_dd4	$x, y, -1+z$	−13.4	11.3	nonspecific
I_dd5	$x, 1+y, 1+z$	−11.2	9.4	nonspecific
I_dd6	$x, -1+y, -1+z$	−11.2	9.4	nonspecific
I_dd7	$1+x, -1+y, z$	−9.7	8.2	nonspecific
I_dd8	$-1+x, 1+y, z$	−9.7	8.2	nonspecific

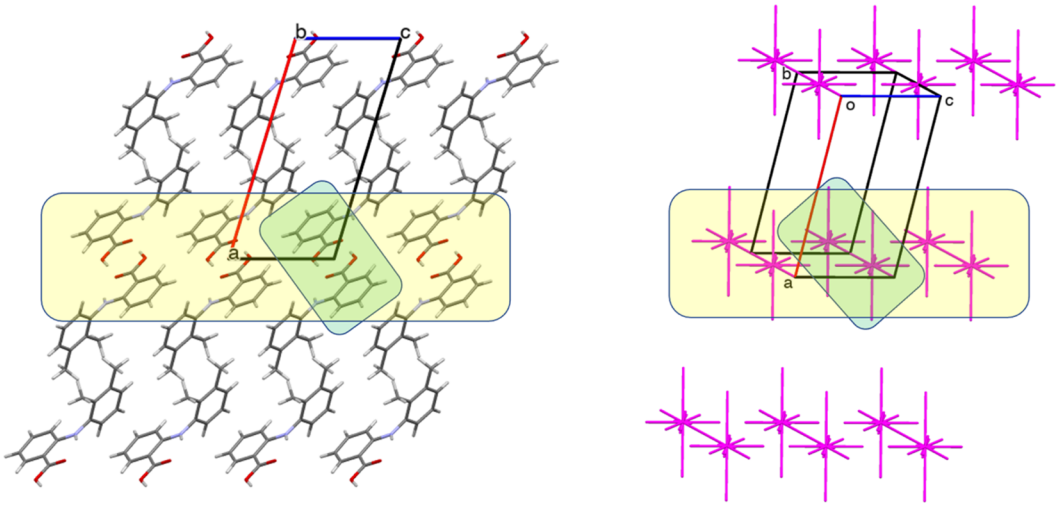

Figure 4. (left) Packing of the polymorphic structure **I** in terms of molecules, projection in the *b* crystallographic direction, and (right) energy-vector diagrams constructed for DBU. Columns are highlighted in green, and layers are highlighted in yellow.

The molecule of mefenamic acid is disordered in structure **II**; therefore, the study of pairwise interaction energies was carried out for each conformer (**A** and **B**) separately. As was mentioned above, these conformers are not equal in the formation of intermolecular interactions with neighboring molecules. However, the strongest interactions are the same; only the weakest interactions differ. Each conformer forms the two strongest interactions in opposite directions, forming a column as the BSM_1 in structure **II** (Table 5 and Figure 5). The interaction energy of each conformer within the column is

https://doi.org/10.1021/acsomega.1c06967
ACS Omega 2022, 7, 17544−17554

Table 5. Symmetry Codes, Bonding Types, Interaction Energies of the Basic dimeric BU_0s with Neighboring ones (E_{int}, kcal/mol) with the Highest Values (More Than 5% of the Total Interaction Energy) and the Contributions of These Energies to the Total Interaction Energy (%) in the Polymorphic Structure II

dimer	symmetry operation	E_{int}, kcal/mol	contribution to the total interaction energy, %	interaction type
		Conformer **A**		
IIA_dd1	1 + *x*, *y*, 1 + *z*	−14.3	12.7	stacking between dimethylphenyl groups
IIA_dd2	−1 + *x*, *y*, −1 + *z*	−14.3	12.7	
IIA_dd3	*x*, 1 + *y*, *z*	−10.0	8.8	stacking between benzoic acid groups
IIA_dd4	*x*, −1 + *y*, *z*	−10.0	8.8	
IIA_dd5	1 + *x*, *y*, *z*	−9.2	8.1	stacking between benzoic acid groups
IIA_dd6	−1 + *x*, *y*, *z*	−9.2	8.1	
IIA_dd7	*x*, *y*, 1 + *z*	−8.7	7.7	nonspecific
IIA_dd8	*x*, *y*, −1 + *z*	−8.7	7.7	nonspecific
IIA_dd9	x, 1 + *y*, −1 + *z*	−8.6	7.6	C−H···π
IIA_dd10	*x*, −1 + *y*, 1 + *z*	−8.6	7.6	C−H···π
		Conformer **B**		
IIB_dd1	1 + *x*, *y*, 1 + *z*	−13.1	11.3	stacking between dimethylphenyl groups
IIB_dd2	−1 + *x*, *y*, 1 + *z*	−13.1	11.3	
IIB_dd3	*x*, 1 + *y*, *z*	−10.0	8.7	stacking between benzoic acid groups
IIB_dd4	*x*, −1 + *y*, *z*	−10.0	8.7	
IIB_dd5	*x*, *y*, 1 + *z*	−9.3	8.0	nonspecific
IIB_dd6	*x*, *y*, −1 + *z*	−9.3	8.0	nonspecific
IIB_dd7	1 + *x*, *y*, *z*	−9.2	8.0	nonspecific
IIB_dd8	−1 + *x*, y,*z*	−9.2	8.0	nonspecific
IIB_dd9	*x*, 1 + *y*, −1 + *z*	−7.0	6.1	nonspecific
IIB_dd10	*x*, −1 + *y*, 1 + *z*	−7.0	6.1	nonspecific

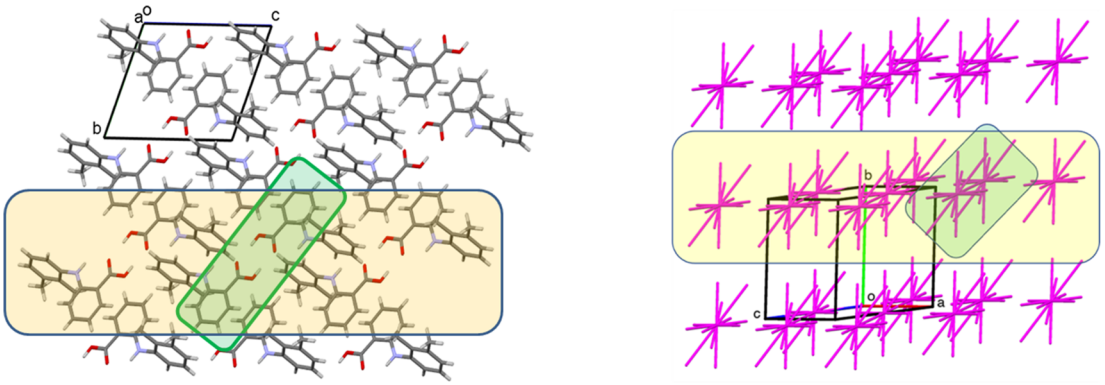

Figure 5. (left) Packing of the polymorphic structure **II** in terms of molecules, projection in the *b* crystallographic direction, and (right) energy-vector diagrams constructed for DBU. Columns are highlighted in green, and layers are highlighted in yellow.

Table 6. Symmetry Codes, Bonding Types, Interaction Energies of the Basic dimeric BU_0s with Neighboring Ones (E_{int}, kcal/mol) with the Highest Values (More Than 5% of the Total Interaction Energy) and the Contributions of These Energies to the Total Interaction Energy (%) in the Polymorphic Structure III

dimer	symmetry operation	E_{int}, kcal/mol	contribution to the total interaction energy, %	i0nteraction type
III_dd1	1 + *x*, −1 + *y*, *z*	−11.2	9.6	stacking between benzoic acid groups
III_dd2	−1 + *x*, 1 + *y*, *z*	−11.2	9.6	
III_dd3	1 + *x*, *y*, *z*	−9.8	8.4	nonspecific
III_dd4	−1 + *x*, *y*, *z*	−9.8	8.4	nonspecific
III_dd5	1 + *x*, *y*, −1 + *z*	−9.0	7.7	nonspecific
III_dd6	−1 + *x*, *y*, 1 + *z*	−9.0	7.7	nonspecific
III_dd7	*x*, 1 + *y*, *z*	−8.7	7.5	nonspecific
III_dd8	*x*, −1 + *y*, *z*	−8.7	7.5	nonspecific
III_dd9	2 + *x*, −1 + *y*, −1 + *z*	−8.5	7.3	nonspecific
III_dd10	−2 + *x*, 1 + *y*, 1 + *z*	−8.5	7.3	nonspecific
III_dd11	1 + *x*, −1 + *y*, −1 + *z*	−6.5	5.6	nonspecific
III_dd12	−1 + *x*, 1 + *y*, 1 + *z*	−6.5	5.6	nonspecific

https://doi.org/10.1021/acsomega.1c06967
ACS Omega 2022, 7, 17544−17554

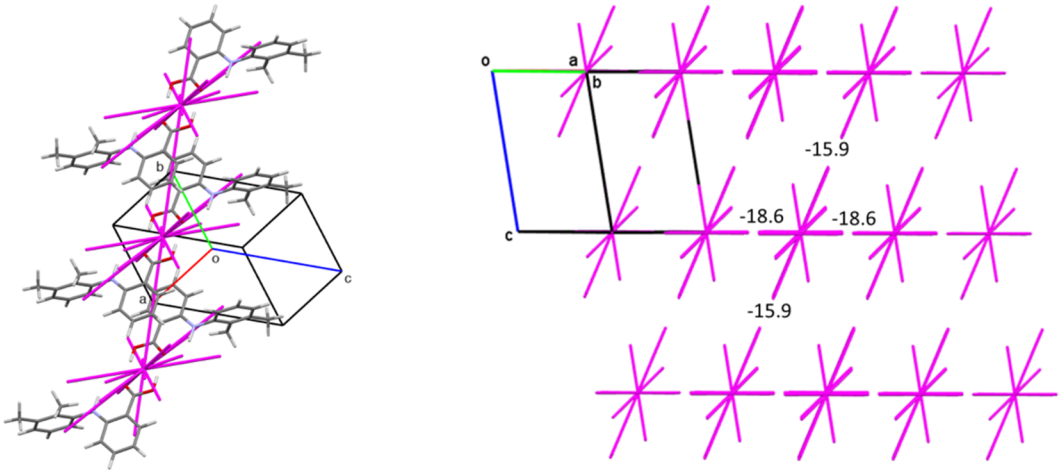

Figure 6. Packing of the polymorphic structure **III**: (left) column as a BSM_1 in terms of molecules and energy-vector diagrams and (right) packing of columns in terms of energy-vector diagrams constructed for the DBU with the interaction energies (in kcal/mol) between the adjacent columns.

−28.6 kcal/mol (conformer **A**) or −26.2 kcal/mol (conformer **B**).

Dimeric building units interact with molecules belonging to neighboring columns with different energies. The strongest interactions between the columns are revealed within the (010) crystallographic plane. The total interaction energy of the DBU_0 with all neighbors within this plane is −66.2 kcal/mol for conformer **A** and −63.2 kcal/mol for conformer **B**, while the interaction energies between adjacent layers are −46.8 and −52.4 kcal/mol for conformers **A** and **B**, respectively. In the case of the other layer parallel to the (−101) crystallographic plane, the interaction energies within the layer and between the neighboring layers are almost equal. Therefore, the layer parallel to the (010) crystallographic plane should be recognized as a BSM_2 in structure **II**. Similarly to structure **I**, the polymorphic form **II** should be classified as columnar-layered. However, the interaction energies between adjacent layers are much stronger in the structure **II** than in the structure **I**.

In the polymorphic structure **III**, the interactions of DBU_0 are stronger in two opposite directions (Table 6), leading to the formation of a column as a BSM_1 (Figure 6). The molecules belonging to neighboring DBUs within this column are bound by the stacking interactions between benzoic acid groups. The interaction energy of the DBU_0 with two neighbors within this column is −22.4 kcal/mol. Interactions of DBU_0 with molecules belonging to neighboring columns are very close in various directions (Table 6). This makes it possible to classify the polymorphic structure **III** as almost isotropic packing of columns (Figure 6).

The results of the study of interaction energies between molecules in the three polymorphic forms of mefenamic acid have been compared with the data about their stabilityies under ambient conditions (**I** > **II** > **III**).[23] The least stable polymorphic form proved to be the most isotropic from the viewpoint of interaction energies (Table 7). The polymorphic forms **I** and **II** have the same packing type (columnar-layered), and the packing of DBUs is more anisotropic in the most stable polymorph **I**. The obtained regularities between crystal structure stability and the degree of its packing anisotropy correlate with previously published data.[35,36]

It should be also noted that the main difference of the polymorphic structure **I** in comparison to structure **II** is the absence or presence of stacking interactions between dimethylphenyl groups (Figure 7). The relative positions of the dimeric building units are very similar in these structures. This similarity makes it possible to assume that the reversible thermal polymorphic transition between these polymorphic structures can be caused by the shift of the DBUs due to a soft enough mild interaction between dimethylphenyl fragments.

Table 7. Comparison of the BU Interactions in the Polymorphic Modifications I−III

param	polymorph **I**	polymorph **II**, **A**/**B**	polymorph **III**
E_{int} within the DBU_0, kcal/mol	−17.4	−17.1/−16.0	−17.7
total E_{int} of DBU_0, kcal/mol	−118.5	−113.0/−115.6	−116.2
E_{int} within BSM_1, kcal/mol	−36.5	−28.6/−26.2	−22.4
E_{int} within BSM_2, kcal/mol	−89.8	−66.2/−63.2	−61.4
BSM_2/BSM_2, kcal/mol	−28.7	−46.8/−52.4	−54.8
packing type	columnar-layered	columnar-layered	columnar

Study of Possible Deformation of Mefenamic Acid Crystals. The existence of a reversible transition between the polymorphic forms **I** and **II** at different temperatures raises the question about the stability of mefenamic acid crystals under pressure. Only polymorphic form **I**, as a commercially available compound, has been studied in a DAC at various pressures up to 2.5 GPa.[22] Unfortunately, full data about the crystal structures obtained at these pressures were not reported. Only the changes in unit cell parameters and volumes were discussed.[22] However, that study revealed there is no polymorphic transition for the polymorphic form **I** of mefenamic acid under pressure. Moreover, structure **I** disintegrates under a pressure of 3.0 GPa.

Previously, we have proposed an approach to determine if a crystal structure can be deformed using quantum chemical modeling.[27,28] Our results of an "energetic" structure of the mefenamic acid polymorphic forms can be used for further modeling. First of all, a preliminary evaluation connected to the possible directions of the shift of strongly bound layers to each other should be carried out. For this purpose, a model system containing one dimeric building unit as a mobile part

https://doi.org/10.1021/acsomega.1c06967
ACS Omega 2022, 7, 17544−17554

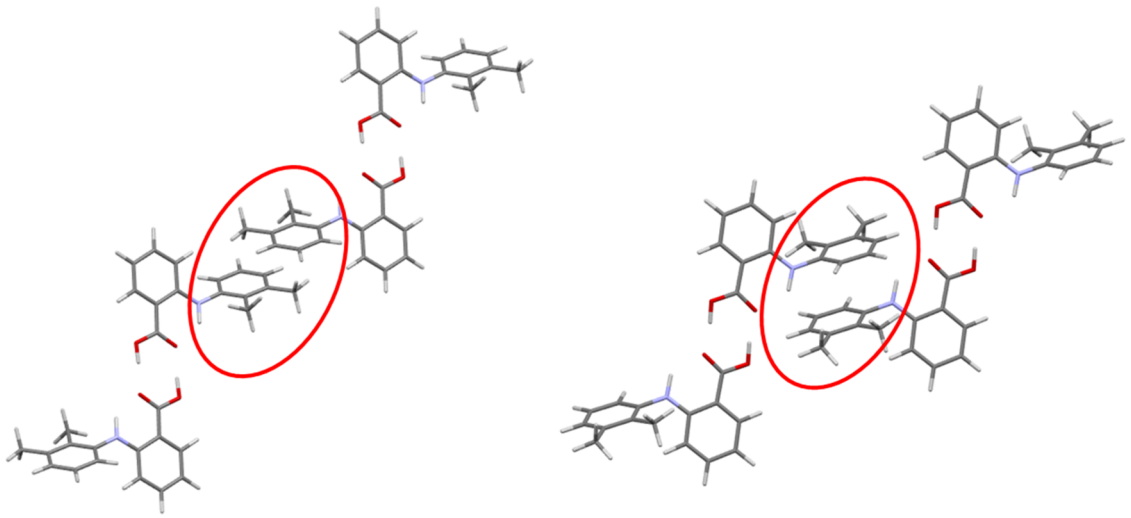

Figure 7. Relative positions of the dimeric building units in the polymorphic structures (left) **I** (on the left) and (right) **II** leading to the absence of a stacking interaction between dimethylphenyl groups (polymorph **I**) and its presence (polymorph **II**).

and a fragment of its neighboring layer as a fixed part was extracted from the crystal structure. The mobile part (DBU) was shifted in relation to the fixed part, and the shortest distances between them were measured at each point. To take into account the nature of the closest atoms, not the shortest distances between atoms but rather the parameter δ was used to construct 2D maps (Figure 8). This parameter shows the difference between the distance and the corresponding van der Waals radii sum.

Since an evaluation of the distances and their comparison with the sum of van der Waals radii does not require complicated calculations and, accordingly, significant computer resources, it seems possible to carry out the preliminary evaluation for all polymorphic forms of mefenamic acid (Figure 8 and Figures S5 and S6).

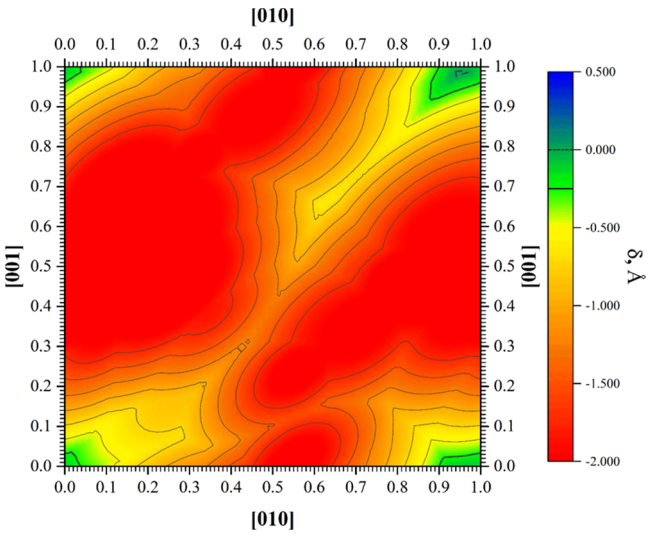

Figure 8. Map of δ (Å) occurring during the shear of the dimeric mobile part in relation to the fixed part in the (100) plane (directions of shift are shown by axes) in the crystal of mefenamic acid polymorphic form **I**. A dashed contour surrounds the zones without the shortening of interatomic distances below the corresponding sum of van der Waals radii (δ). A bold contour surrounds zones with δ values smaller than −0.25 Å.

As can be seen from the 2D map corresponding to the shift of the layers parallel to the (100) crystallographic plane (Figure 8), no region with the parameter $\delta \geq 0$ can be found in structure **I**. This means that any shift of two neighboring layers to each other leads to an approach of molecules and a significant increase in interaction energies between them up to positive values. The same results were obtained for the polymorphic forms **II** and **III** (Figures S5 and S6).

A modeling of the shear deformation and calculations of the interaction energies between the mobile and fixed parts of the model system was performed for the displacement on one crystallographic translation in the [010], [001], and [011] crystallographic directions within the layer parallel to the (100) crystallographic plane in structure **I**, which is commercially available. These calculations revealed extremely high energy barriers (more than 400 kcal/mol) for the displacements in the [010] and [001] directions (Figure 9). Moreover, our attempts to calculate interaction energies for several points in a region of an expected energy maximum have failed due to very short distances between the molecules of the mobile and fixed parts.

The displacement of the mobile part in the [011] diagonal crystallographic direction along the (100) crystallographic plane looks to be more probable (Figure 10). The full energy profile for this displacement was constructed using the results of interaction energy calculations. The detailed analysis of this energy profile has not revealed any local minimum in the region of a starting point that was declared as a precondition, indicating the possibility of a polymorphic transition in piracetam crystals.[28] The energy barrier for the displacement in the [011] direction was estimated to be 164.1 kcal/mol, which is also very high.

Thus, quantum chemical modeling of the shear deformation in the polymorphic structure **I** of mefenamic acid has not revealed structural features that can be considered as preconditions for a polymorphic transition under pressure.

CONCLUSIONS

The application of modern quantum chemical methods to an analysis of the crystal structures of three mefenamic acid polymorphic modifications allows obtaining much more information in comparison to the usual experimental data. It was revealed that two O−H···O hydrogen bonds between

https://doi.org/10.1021/acsomega.1c06967
ACS Omega 2022, 7, 17544−17554

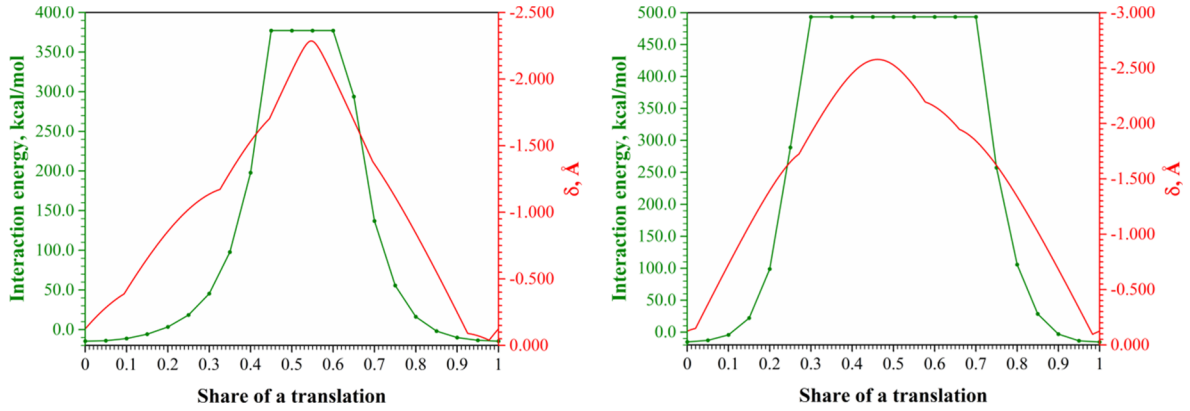

Figure 9. Profiles of interaction energy (green line) and the topological parameter δ (red line) occurring during the shear of the dimeric building unit along the neighboring layer (100) (left) in the [010] crystallographic direction and (right) in the [001] crystallographic direction in the crystals of the mefenamic acid polymorphic modification **I** under ambient pressure.

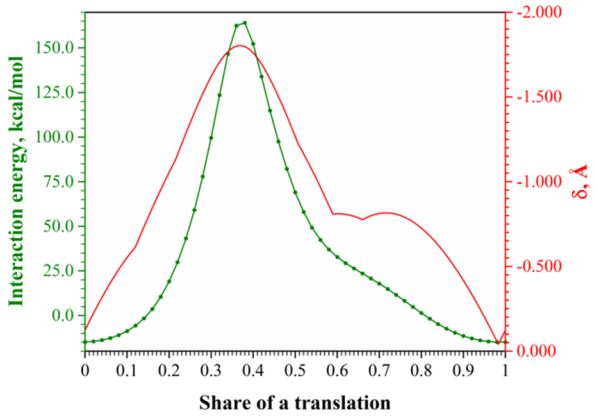

Figure 10. Profiles of interaction energy (green line) and the topological parameter δ (red line) occurring during the shear of the dimeric building unit along the neighboring layer (100) in the [011] crystallographic direction in the crystals of the mefenamic acid polymorphic modification **I** under ambient pressure.

carboxylic groups form a centrosymmetric dimer as a complex building unit in all of these structures but do not give any information about a crystal packing type. The study of the pairwise interaction energies between molecules showed that polymorphic forms **I** and **II** have a columnar-layered structure while that of polymorphic form **III** is columnar. Columns as a BSM_1 are formed due to the stacking interactions between benzoic acid fragments in all of the structures under study. In structures **I** and **II**, the columns are bound more strongly in two opposite directions, forming a layer parallel to the crystallographic plane (100) in **I** or (010) in **II** as a BSM_2. The interactions between dimeric building units within the layer are stronger and those between neighboring layers are weaker in the most stable polymorphic form **I**.

Shear deformation modeling of the strongly bound layers has been performed using an approach proposed recently.[27,28] A preliminary assessment of the shear deformation using the parameter δ, which shows how the distance between the closest atoms of the mobile and fixed parts of the model system differs from the corresponding van der Waals radii sum, was made for all the polymorphic structures of mefenamic acid. This assessment revealed that a deformation of these structures is hardly possible.

A detailed study of the displacement of the mobile part in relation to the fixed part along the (100) crystallographic layer recognized as BSM_2 was performed for the commercially available polymorphic form **I**, for which the experimental data were obtained using a diamond anvil cell (DAC).[22] Quantum chemical calculations did not reveal any prerequisites indicating the possibility of a polymorphic transition under pressure that were found in piracetam crystals. In the polymorphic structure **I**, there is no local minimum near the starting point and a shift in the energy barrier is extremely high.

EXPERIMENTAL SECTION

Molecular Structure Study. The scanning of the torsion angles was performed using density functional theory with the m06-2x functional[37] and standard cc-pVTZ basis set[38] (m06-2x/cc-pVTZ). The energy barriers for rotation around the $C_{ar}-N-C_{ar}-C_{ar}$ torsion angle were calculated as the difference between the energies of the true minima and saddle point geometrical structures. All calculations were performed using the Gaussian09 program.[39]

Crystal Structure Analysis. The data on the crystal structures of the mefenamic acid polymorphic forms **I**–**III** (XYANAC,[5] XYANAC05,[21] XYANAC03[23]) studies were extracted from the Cambridge Structural Database.[40] These structures were analyzed using quantum chemical calculations of the pairwise interaction energies between molecules.[32−34] According to this approach, the following operations have been performed:

(1) The first coordination sphere of a basic molecular building unit (MBU_0) or dimeric building unit (DBU_0) has been determined using the "Molecular Shell calculation" option within the Mercury program.[41]

(2) Positions of hydrogen atoms were shifted to their standard neutron values.[42]

(3) The E_i energies of an intermolecular interaction of a BU_0 with one of its nearest neighbors were calculated using the B97-D3/def2-TZVP density functional method[43−45] and corrected for basis set superposition error using the counterpoise procedure.[46]

(4) The calculated interaction energies have been visualized using energy vector diagrams.[33] All of the calculations were performed within the ORCA program.[47] More

https://doi.org/10.1021/acsomega.1c06967
ACS Omega 2022, 7, 17544−17554

detailed descriptions of this approach can be found in previous publications.[27,28,48]

Quantum Chemical Modeling of Shear Deformation. To study the possibility of shear deformation, a model system containing one building unit as a mobile part and a fragment of a neighboring layer as a fixed part was extracted from the experimental crystal structure. According to the method proposed previously,[27] shear deformation is possible due to the displacement of strongly bound fragments of a crystal packing to each other. Using an approximation of a rigid body, it was assumed that these fragments have to be unchanged during the displacement. The procedure had two steps.

Step 1: Preliminary Assessment of Shear Deformation Possibility..[28,48] A mobile part of the model system was shifted in relation to the fixed part, and the minimum interatomic distances between the closest atoms were determined. To take into account the nature of atoms, the difference in interatomic distances and corresponding van der Waals radii sum (the parameter δ) was calculated at each point. The step size for the translation at this studying step was picked up to reach a resolution of 0.010 Å for every possible shift direction.

The maximum value of the parameter δ indicates the absence of any steric repulsion between the mobile and fixed parts of the model system and shows a possible direction for shear deformation.

Step 2: Study of Energetic Characteristics of Shear Deformation in the Most Probable Directions. The model system used at the previous step was extended by one additional translation in directions collinear and anticollinear to the displacement vector to take into account an edge effect. The mobile part of the model system was shifted along the fixed part by one crystallographic translation, and the single-point interaction energies between the mobile and fixed fragments were calculated at each point along a translation trajectory. The step size for this shift was set equal to 0.05 of a translation for the directions [010] and [001] and 0.02 of a translation for the direction [011]. These distances between the computational points were chosen as the largest step size with good reproducibility in comparison to that of 0.001 of a translation (Table S8).

The interaction energies between the mobile and fixed parts were calculated at each point using the B97-D3 method and cc-PVDZ basis set.[49,50] All calculations were performed using the Gaussian09 software package.[39] The shift energy profile was constructed as a function of the calculated interaction energy and the shift of the mobile part in relation to the initial position. The shift energy barrier was calculated as the difference between the highest and lowest interaction energies between the mobile and fixed parts within a translation.

■ ASSOCIATED CONTENT

Supporting Information

The Supporting Information is available free of charge at https://pubs.acs.org/doi/10.1021/acsomega.1c06967.

Full tables of the pairwise interactions energie between molecules and figures of the crystal packing along different crystallographic directions in terms of molecules and energy-vector diagrams (PDF)

■ AUTHOR INFORMATION

Corresponding Author

Svitlana V. Shishkina − *SSI Institute for Single Crystals NAS of Ukraine, Department of X-ray Diffraction Study and Quantum Chemistry, Kharkiv 61001, Ukraine;* orcid.org/0000-0002-3946-1061; Phone: +38 066 771 87 42; Email: sveta12.20@gmail.com, sveta@xray.isc.kharkov.com

Authors

Yevhenii A. Vaksler − *SSI Institute for Single Crystals NAS of Ukraine, Department of X-ray Diffraction Study and Quantum Chemistry, Kharkiv 61001, Ukraine*

Irina S. Konovalova − *SSI Institute for Single Crystals NAS of Ukraine, Department of X-ray Diffraction Study and Quantum Chemistry, Kharkiv 61001, Ukraine;* orcid.org/0000-0001-6245-6642

Victoriya V. Dyakonenko − *SSI Institute for Single Crystals NAS of Ukraine, Department of X-ray Diffraction Study and Quantum Chemistry, Kharkiv 61001, Ukraine*

Victoriya V. Varchenko − *SSI Institute for Single Crystals NAS of Ukraine, Department of X-ray Diffraction Study and Quantum Chemistry, Kharkiv 61001, Ukraine;* orcid.org/0000-0002-7369-1637

Complete contact information is available at: https://pubs.acs.org/10.1021/acsomega.1c06967

Author Contributions

S.V.S. analyzed the results and wrote the manuscript. Y.A.V. performed quantum chemical calculations and analyzed the results. I.S.K. performed quantum chemical calculations and discussed the results. V.V.D. performed quantum chemical calculations. V.V.V. discussed the results.

Funding

The work was supported by the grant of the National Research Foundation of Ukraine 2020.02/0183.

Notes

The authors declare no competing financial interest.

■ REFERENCES

(1) Flower, R. J. Drugs which inhibit prostaglandin biosynthesis. *Pharmacol. Rev.* **1974**, *26*, 33−67.

(2) Dhanaraj, V.; Vijayan, M. Structural studies of analgesics and their interactions. XII. Structure and interactions of anti-inflammatory fenamates. A concerted crystallographic and theoretical conformational study. *Acta Cryst., Sect. B: Struct. Sci., Cryst. Eng. Mater.* **1988**, *B44*, 406−412.

(3) Lozano, J. J.; Pouplana, R.; López, M.; Ruiz, J. Conformational analysis of the anti- inflammatory fenamates: a molecular mechanics and semiempirical molecular orbital study. *J. Mol. Struct. (Theochem)* **1995**, *335*, 215−227.

(4) Uzoh, O. G.; Galek, P. T. A.; Price, S. L. Analysis of the conformational profiles of fenamates shows route towards novel, higher accuracy, force-fields for pharmaceuticals. *Phys. Chem. Chem. Phys.* **2015**, *17*, 7936−7948.

(5) McConnell, J. F.; Company, F. Z. N-(2,3-xylyl)anthranilic acid, $C_{15}H_{15}NO_2$. Mefenamic acid. *Cryst. Struct. Commun.* **1976**, *5*, 861−864.

(6) Lee, E. H.; Byrn, S. R.; Carvajal, M. T. Additive-induced metastable single crystal of a mefenamic acid. *Pharm. Res.* **2006**, *23*, 2375−2380.

(7) Cesur, S.; Gokbel, S. Crystallization of mefenamic acid and polymorphs. *Cryst. Res. Technol.* **2008**, *43* (7), 720−728.

(8) Nicholson, C. E.; Cooper, S. J. Crystallization of mefenamic acid from dimethylformamide microemulsions: obtaining thermodynamic control through 3D nanoconfinement. *Crystals* **2011**, *1*, 195−205.
(9) Abdul Mudalip, A. K.; Abu Bakar, M. R.; Jamal, P.; Adam, F.; Che Man, R.; Sulaiman, S. Z.; Mohd Arshad, Z. I.; Md. Shaarani, S. Effects of solvents on polymorphism and shape of mefenamic acid crystals. *MATEC Web of Conferences* **2018**, *150*, 02004.
(10) Aguiar, A. J.; Zelmer, J. E. Dissolution behavior of polymorphs of chloramphenicol palmitate and mefenamic acid. *J. Pharm. Sci.* **1969**, *58* (8), 983−987.
(11) Romero, S.; Escalera, B.; Bustamante, P. Solubility behavior of polymorphs I and II of mefenamic acid in solvent mixtures. *Int. J. Pharm.* **1999**, *178*, 193−202.
(12) Abdul Mudalip, S. K.; Abu Bakar, M. R.; Jamal, P.; Adam, F. Solubility and dissolution thermodynamical data of mefenamic acid crystals in different classes of organic solvents. *J. Chem. Eng. Data* **2013**, *58*, 3447−3452.
(13) Panchagnula, R.; Sundaramurthy, P.; Pillai, O.; Agrawal, S.; Raj, Y. A. Solid-state characterization of mefenamic acid. *J. Pharm. Sci.* **2004**, *93* (4), 1019−1029.
(14) Gilpin, R. K.; Zhou, W. Infrared studies of the polymorphic states of the fenamates. *J. Pharm. Biomed. Anal.* **2005**, *37*, 509−515.
(15) Jabeen, S.; Dines, T. J.; Leharne, S. A.; Chowdhry, B. Z. Raman and IR spectroscopic studies of fenamates − conformational differences in polymorphs of flufenamic acid, mefenamic acid and tolfenamic acid. *Spectrochim. Acta, Part A* **2012**, *96*, 972−985.
(16) Cunha, V. R. R.; Izumi, C. M. S.; Petersen, P. A. D.; Magalhães, A.; Temperini, M. L. A.; Petrilli, H. M.; Constantino, V. R. L. Mefenamic acid anti-inflammatory drug: probing ots polymorphs by vibrational (IR and Raman) and solid-state NMR spectroscopies. *J. Phys. Chem. B* **2014**, *118*, 4333−4344.
(17) Antonio, M.; Maggio, R. M. Assessment of mefenamic acid polymorphs in commercial tablets using chemometric coupled to MIR and NIR spectroscopies. Prediction of dissolution performance. *J. Pharm. Biomed. Anal.* **2018**, *149*, 603−611.
(18) Gilpin, R. K.; Zhou, W. Infrared studies of the thermal conversion of mefenamic acid between polymorphic states. *Vib. Spectrosc.* **2005**, *37*, 53−59.
(19) Kato, F.; Otsuka, M.; Matsuda, Y. Kinetic study of the transformation of mefenamic acid polymorphs in various solvents and under high humidity conditions. *Int. J. Pharm.* **2006**, *321*, 18−26.
(20) Surov, A. O.; Terekhova, I. V.; Bauer-Brandi, A.; Perlovich, G. L. Thermodynamic and structural aspects of some fenamate molecular crystals. *Cryst. Growth Des.* **2009**, *9* (7), 3265−3272.
(21) Yang, X.; Sarma, B.; Myerson, A. S. Polymorph control of micro/nano-sized mefenamic acid crystals on patterned self-assembled monolayer islands. *Cryst. Growth Des.* **2012**, *12*, 5521−5528.
(22) Abbas, N.; Oswald, I. D. H.; Pulham, C. R. Accessing mefenamic acid form II through high-pressure recrystallization. *Pharmaceutics* **2017**, *9*, 16.
(23) SeethaLekshmi, S.; Guru Row, T. N. Conformational polymorphism in a non-steroidal anti-inflammatory drug, mefenamic acid. *Cryst. Growth Des.* **2012**, *12*, 4283−4289.
(24) Pang, Y.; Buanz, A.; Telford, R.; Magdysyuk, O. V.; Gaisford, S.; Williams, G. R. A simultaneous X-ray diffraction-differential scanning calorimetry study into the phase transitions of mefenamic acid. *J. Appl. Crystallogr.* **2019**, *52*, 1264−1270.
(25) Shishkin, O. V.; Zubatyuk, R. I.; Shishkina, S. V.; Dyakonenko, V. V.; Medviediev, V. V. Role of supramolecular synthons in the formation of the supramolecular architecture of molecular crystals revisited from an energetic viewpoint. *Phys. Chem. Chem. Phys.* **2014**, *16*, 6773−6786.
(26) Shishkina, S. V. Using of quantum-chemical calculations to molecular crystal studying. *Struct. Chem.* **2019**, *30*, 1565−1577.
(27) Vaksler, Ye.; Idrissi, A.; Urzhuntseva, V. V.; Shishkina, S. V. Quantum chemical modeling of mechanical properties of aspirin polymorphic modifications. *Cryst. Growth Des.* **2021**, *21* (4), 2176−2186.
(28) Vaksler, Ye.; Idrissi, A.; Shishkina, S. V. High-pressure influence on piracetam crystals: studying by quantum chemical methods. *Cryst. Growth Des.* **2021**, *21* (10), 5697−5711.
(29) Case, D. H.; Srirambhatla, V. K.; Guo, R.; Watson, R. E.; Price, L. S.; Polyzois, H.; Cockcroft, J. K.; Florence, A. J.; Tocher, D. A.; Price, S. L. *Cryst. Growth Des.* **2018**, *18* (9), 5322−5331.
(30) Desiraju, G. R. Supramolecular synthons in crystal engineering − a new organic synthesis. *Angew. Chem., Int. Ed. Engl.* **1995**, *34*, 2311−2327.
(31) Desiraju, G. R. Chemistry beyond the molecule. *Nature* **2001**, *412*, 397−400.
(32) Shishkin, O. V.; Dyakonenko, V. V.; Maleev, A. V.; Schollmeyer, D.; Vysotsky, M. O. Columnar supramolecular architecture of crystals of 2-(4-iodophenyl)-1,1— phenantroline derived from values of intermolecular interaction energy. *CrystEngComm* **2011**, *13*, 800−805.
(33) Shishkin, O. V.; Dyakonenko, V. V.; Maleev, A. V. Supramolecular architecture of crystals of fused hydrocarbons based on topology of intermolecular interactions. *CrystEngComm* **2012**, *14*, 1795−1804.
(34) Shishkin, O. V.; Zubatyuk, R. I.; Maleev, A. V.; Boese, R. Investigation of topology of intermolecular interactions in the benzene-acetylene co-crystal by different theoretical methods. *Struct. Chem.* **2014**, *25*, 1547−1552.
(35) Shishkina, S. V.; Baumer, V. N.; Khromileva, O. V.; Kucherenko, L. I.; Mazur, I. A. The formation of two thiotriazoline polymorphs: study from the energetic viewpoint. *CrystEngComm* **2017**, *19*, 2394−2401.
(36) Shishkina, S. V.; Baumer, V. N.; Kovalenko, S. M.; Trostianko, P. V.; Bunyatyan, N. D. Usage of quantum chemical methods to understand the formation of concomitant polymorphs of acetyl 2-(*N*-(2-fruorophenyl)imino)coumarin-3-carboxamide. *ASC Omega* **2021**, *6* (4), 3120−3129.
(37) Zhao, Y.; Truhlar, D. G. The M06 suite of density functionals for main group thermochemistry, thermochemical kinetics, noncovalent interactions, excited states, and transition elements: two new functionals and systematic testing of four M06-class functionals and 12 other functionals. *Theor. Chem. Acc.* **2008**, *120*, 215−241.
(38) Kendall, R. A.; Dunning, T. H., Jr.; Harrison, R. J. Electron affinities of the first-row atoms revisited. Systematic basis sets and wave functions. *J. Chem. Phys.* **1992**, *96*, 6796−6806.
(39) Frisch, M. J.; Trucks, G. W.; Schlegel, H. B.; Scuseria, G. E.; Robb, M. A.; Cheeseman, J. R., et al. *Gaussian 09, Rev. B.01*; Gaussian, Inc.: 2010.
(40) Groom, C. R.; Bruno, I. J.; Lightfoot, M. P.; Ward, S. C. The Cambridge Structural Database. *Acta Cryst., Sect. B: Struct. Sci., Cryst. Eng. Mater.* **2016**, *B72*, 171−179.
(41) Macrae, C. F.; Bruno, I. J.; Chisholm, J. A.; Edgington, P. R.; McCabe, P.; Pidcock, E.; Rodriguez-Monge, L.; Taylor, R.; van de Streek, J.; Wood, P. A. Mercury CSD 2.0 − new features for the visualization and investigation of crystal structures. *J. Appl. Crystallogr.* **2008**, *41*, 466−470.
(42) Allen, F. H.; Bruno, I. J. Bond lengths in organic and metal-organic compounds revisited: *X*−H bond lengths from neutron diffraction data. *Acta Cryst., Sect. B: Struct. Sci., Cryst. Eng. Mater.* **2010**, *B66*, 380−386.
(43) Grimme, S. Semiempirical GGA-type density functional constructed with a long-range dispersion correction. *J. Comput. Chem.* **2006**, *27*, 1787−1799.
(44) Grimme, S.; Ehrlich, S.; Goerigk, L. Effect of the damping function in dispersion corrected density functional theory. *J. Comput. Chem.* **2011**, *32*, 1456−1465.
(45) Grimme, S.; Antony, J.; Ehrlich, S.; Krieg, H. A consistent and accurate *ab initio* parametrization of density functional dispersion correction (DFT-D) fort he 94 elements H- Pu. *J. Chem. Phys.* **2010**, *132*, 154104.
(46) Boys, S. F.; Bernardi, F. The calculation of small molecular interactions by the differences of separate total energies. Some procedures with reduced errors. *Mol. Phys.* **1970**, *19*, 553−566.

https://doi.org/10.1021/acsomega.1c06967
ACS Omega 2022, 7, 17544−17554

(47) Neese, F. *ORCA 2.8.0*; Universitaet Bonn: 2010.
(48) Vaksler, Ye. A.; Idrissi, A.; Shishkina, S. V. Is it possible to predict the stability of a crystal structure under the influence of pressure? Quantum chemical study of ibuprofen crystals. *New J. Chem.* **2022**, *46*, 3856−3865.
(49) Davidson, E. R. Comment on "Comment on Dunning's correlation-consistent basis sets. *Chem. Phys. Lett.* **1996**, *260*, 514−518.
(50) Dunning, T. H., Jr. Gaussian basis sets for use in correlated molecular calculations. I. The atoms boron through neon and hydrogen. *J. Chem. Phys.* **1989**, *90*, 1007−1023.

https://doi.org/10.1021/acsomega.1c06967
ACS Omega 2022, 7, 17544−17554